Journal of Solid State Chemistry 186 (2012) 240–246

Contents lists available at SciVerse ScienceDirect

Journal of Solid State Chemistry

journal homepage: www.elsevier.com/locate/jssc

Structural and physical properties of Re substituted *B*-site ordered and disordered $SrCo_{1-x}Re_xO_{3-\delta}$ ($x=0.1$, 0.25, 0.5)

A. Baszczuk [a,*], B. Dabrowski [b,c], S. Kolesnik [b,c], O. Chmaissem [b,c], M. Avdeev [d]

[a] Wroclaw University of Technology, Institute of Materials Science and Applied Mechanics, 50-370 Wroclaw, Poland
[b] Department of Physics, Northern Illinois University, DeKalb, IL 60115, USA
[c] Materials Science Division, Argonne National Laboratory, Argonne, IL 60439, USA
[d] Bragg Institute, Australian Nuclear Science and Technology Organization, Menai, NSW 2234, Australia

ARTICLE INFO

Article history:
Received 23 July 2011
Received in revised form
6 November 2011
Accepted 11 December 2011
Available online 19 December 2011

Keywords:
Perovskite
Magnetic structure
Rietveld analysis
Neutron powder diffraction
Antiferromagnetic
Cation ordering

ABSTRACT

Synthesis conditions, structural, magnetic and transport properties have been studied for $SrCo_{1-x}Re_xO_{3-\delta}$ samples with $x=0.1$, 0.25, 0.5. $SrCo_{0.9}Re_{0.1}O_{3-\delta}$ forms in air and remains stable on cooling indicating that small amounts of Re^{7+} stabilize a *B*-site disordered *Pm*-3*m* phase inhibiting formation of a hexagonal phase observed for $SrCoO_{3-\delta}$. After oxygenation $SrCo_{0.9}Re_{0.1}O_{2.94}$ becomes ferromagnetic below 125 K and shows metallic-like conductivity with moderate magnetoresistance at low temperatures. Fully oxygenated double perovskite Sr_2CoReO_6 ($x=0.5$) forms under reducing conditions and is tetragonal at room temperature. A hysteretic transition to the antiferromagnetic state at low temperatures (~50–60 K) is coupled with a drastic change of electronic and thermal properties. Contrary to previous reports [A. Nag et al., Chem. Mater. 20(13) (2008) 4420–4424] $SrCo_{0.75}Re_{0.25}O_3$ is not a partially cation ordered $Sr_4Co_3ReO_{12}$ phase, but a mixture of two structural and magnetic phases with disordered $SrCo_{1-xd}Re_{xd}O_3$ and ordered $SrCo_{1-xo}Re_{xo}O_3$ compositions where $xd > 0.1$ and $xo < 0.5$.

1. Introduction

Pure and substituted $SrCoO_{3-\delta}$ perovskites are of considerable current interest due to thermally induced changes of cobalt spin configurations [1,2] that lead to a rich variety of magnetic and transport properties sensitive to charge doping and crystal structure [3–6]. The parent $SrCoO_{3-\delta}$ material displays also high oxygen mobility near room temperature [7–11] that makes it very suitable for several technical applications such as gas sensing probes, oxygen membranes and components of solid oxide fuel cells. $SrCoO_{3-\delta}$ crystallizes in various structures depending on the oxygen content and temperature. It was shown [12] that compound with approximate stoichiometry $Sr_2Co_2O_5$ (or $SrCoO_{2.5}$) exists in air in three different polymorphs: (i) an orthorhombic brownmillerite phase between room temperature and 653 °C, (ii) a non-perovskite hexagonal phase between 653 and 920 °C and (iii) a cubic perovskite phase above 920 °C, which transforms irreversibly back to the hexagonal phase below 774 °C when cooled. High-temperature $SrCoO_{3-\delta}$ polymorph phases with cubic 3C-like crystal structures are mixed ionic–electronic conductors that exhibit some of the highest electrical conductivity and oxygen permeability values [12], yet structural instabilities limit potential applications of this material. Therefore, it is extremely important to find an effective way to stabilize the cubic phase at high temperatures for mixed ionic–electronic applications and at room and low temperatures for studies of magnetic and transport properties.

The room temperature oxygen contents and crystal structures of $SrCoO_{3-\delta}$-based compounds can be controlled by synthesis and chemical substitution procedures. Fast cooling from high temperatures hinders formation of the hexagonal phase ensuing a highly oxygen deficient perovskite phase. If the synthesis is carried out under high-pressure conditions (~6 GPa) full oxygen stoichiometry of 3.0 can be achieved [13,14]; thus, resulting in a simple cubic perovskite structure. Fully oxygen stoichiometric perovskites can also be obtained by low-temperature electrochemical oxidation of the $SrCoO_{2.5}$ brownmillerite [15]. The introduction of a heterovalent cation on the strontium and/or cobalt sites also allows for the stabilization of the stoichiometric perovskite structure [3–6,16,17]. Among all dopants introduced into the *B* site iron is one of the most interesting. The cobalt and iron based perovskite oxides have been shown to be some of the most attractive materials for mixed ionic–electronic applications [18]. Several substitutions of quadri- or pentavalent ions have been studied [19–21], but only few studies have been devoted to materials where cobalt is substituted by even higher oxidation state ions.

* Corresponding author.
E-mail address: agnieszka.baszczuk@pwr.wroc.pl (A. Baszczuk).

0022-4596/$ - see front matter © 2011 Elsevier Inc. All rights reserved.
doi:10.1016/j.jssc.2011.12.017

Among the various metal cations that can be substituted for cobalt, rhenium is worth investigating because its 7+ valence found in oxides should allow stoichiometric perovskite structures to form at relatively low substitution levels. In addition, when compared to 3*d* transition metal oxides, the 4*d* and 5*d* counterparts have thus-far been much less explored. The 4*d* and 5*d* transition metal oxides exhibit different crystal structures and crystal chemistry from 3*d* oxides owing to the more extended nature of the 4*d* and 5*d* orbitals, the predominance of higher oxidation states and a tendency to form metal–metal bonds, among others [22]. The magnetism of the Re 5*d* electrons has recently attracted considerable attention. For example, Sr_2FeReO_6, exhibiting the metal–insulator transition [23] and the superconducting $Cd_2Re_2O_7$ [24] and $Hg(x)ReO_3$ [25] have been the subject of several recent studies. Rhenium-containing cobalt perovskites with compositions Sr_2CoReO_6 and $Sr_4Co_3ReO_{12}$ have been previously described by Kato et al. [26], Retuerto et al. [27] and Nag et al. [28], respectively. Sr_2CoReO_6 was characterized as a tetragonal (*I*4/*m*) double perovskite antiferromagnet with $T_N=60$ K [26,27] while $Sr_4Co_3ReO_{12}$ was described as a $T_C=250$ K ferromagnet that crystallizes in a partially ordered double perovskite (*Fm*-3*m*) structure [28].

In this publication, we report on the synthesis, structure, and physical properties of the $SrCo_{1-x}Re_xO_{3-\delta}$ series with $x=0.1$, 0.25, 0.5. It is shown that the presence of rhenium not only helps in stabilizing the perovskite structure, but also enables the full oxygen stoichiometry to be obtained without high oxygen pressure or electrochemical oxidation. We also show that $SrCo_{0.75}Re_{0.25}O_3$ does not form as a *B*-site ordered $Sr_4Co_3ReO_{12}$ phase. Instead, a miscibility gap is identified and the material forms as a mixture of two structural and magnetic phases with approximate compositions of $SrCo_{1-xd}Re_{xd}O_3$ and $SrCo_{1-xo}Re_{xo}O_3$ where $xd>0.1$ and $xo<0.5$ (where *xd* and *xo* refer to disordered and ordered *x*-values, respectively).

2. Synthesis and thermogravimetric characterization

Polycrystalline samples of $SrCo_{1-x}Re_xO_{3-\delta}$ with $x=0.1$, 0.25, 0.5 were synthesized by a solid-state reaction of appropriate amounts of Re_2O_7, Co_3O_4 and $SrCO_3$ (all >99.99% purity). Reactants were thoroughly mixed in an agate mortar and fired several times in air in the 900–1250 °C range with intermediate grindings. The reaction progress was monitored by X-ray diffraction (XRD) performed after each step of the synthesis procedure using a Rigaku D/MAX powder diffractometer in the 10–90° range with Cu*K*α radiation. The $x=0.1$ sample was obtained single-phase after synthesis in air at 1085 °C followed by slow cooling to room temperature indicating that no irreversible transformation to the hexagonal phase is present. The $x=0.5$ sample showed non-perovskite impurities after synthesis in air at any temperature up to 1250 °C. However, synthesis in Ar atmosphere (~20 ppm O_2) immediately resulted in a single-phase material at 1160–1230 °C. The $x=0.25$ sample appeared as a mixture of the *B*-site ordered and disordered phases after synthesis in air at 1200 °C followed by slow cooling contrary to report of Nag et al. [28]. Oxygen deficient sample obtained from air at 1200 °C followed by fast cooling appeared initially as a possibly single-phase *Fm*-3*m* structure, however after annealing in oxygen at 500 °C that sample showed clear mixture of the *B*-site ordered and disordered phases. In many attempts to produce either single-phase disordered material or the partially ordered *Fm*-3*m* structure, the $x=0.25$ sample was annealed at high temperatures of 900–1090 °C in several oxygen atmospheres: high-pressure oxygen, oxygen and pure argon followed by oxygenation at 500 °C. None of these procedures changed the constitution of that sample, however, some variation of the phase fractions was observed as a slight change of the diffraction peak positions and the ratio of peak intensities. The smallest amount of phase separation to the *B*-site ordered and disordered phases after oxygen annealing was observed for the sample from firing in Ar at 1090 °C. Fig. 1 shows typical laboratory X-ray diffraction patterns for selected samples. The persistent presence of the *B*-site ordered phase in the $x=0.25$ sample after synthesis under various conditions that included both high oxygen pressure and pure oxygen under which the $x=0.5$ composition is not stable indicates that the Re content of the *B*-site ordered phase is less than 0.5, i.e., there exists some solubility of the Co antisite defects on the Re sites that stabilizes the *I*4/*m* tetragonal structure under oxidizing conditions.

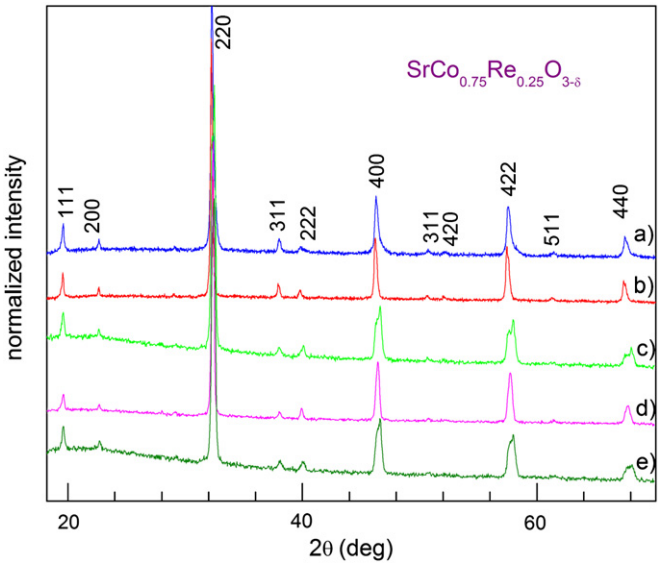

Fig. 1. Room temperature X-ray diffraction patterns of the samples obtained from several annealing conditions: (a) Ar 1090+Ox 400, (b) Ar 1090, (c) Air 1200 slow cool, (d) Air 1200 fast cool, and (e) Air 1200 fast cool+Ox 500. The reflection indices for the double cubic cell are shown.

Several batches of $SrCo_{0.9}Re_{0.1}O_{3-\delta}$, each differing in the oxygen stoichiometry, were obtained by additional annealing. Samples with the lowest oxygen vacancy content ($\delta=0.06$) were obtained by annealing in high-pressure oxygen (250 atm.) at 500 °C followed by a very slow (0.1 °C/min) cooling to room temperature. The sample with $\delta=0.48$ was obtained by heating in Ar at 1095 °C followed by fast cooling to room temperature. Final determination of the oxygen content was performed by thermogravimetric analysis (TGA) performed on a Cahn TG171 thermobalance, considering the weight difference between the initial samples and the total reduction products to SrO and metallic Co and Re (confirmed by XRD) obtained by a slow (1°/min) reduction in a H_2/Ar atmosphere up to the point of no weight change. The remaining samples were obtained by TGA annealing in several flowing gas mixtures up to 1100 °C. Heating the material in pure oxygen, air, and 1%O_2/Ar produced samples with oxygen deficiencies $\delta=0.09$, 0.13 and 0.15, respectively. Fig. 2 shows TGA data for the $x=0.1$ sample obtained on cooling in various atmospheres.

After a conventional solid state synthesis in air and argon, the $x=0.25$ and 0.5 samples were annealed on TGA in pure oxygen at 400 °C followed by very slow cooling to room temperature. The oxygen content in the $x=0.5$ sample did not change showing that the material is fully stoichiometric in Ar at high temperatures of 1200 °C. Annealing the sample in oxygen at 800 °C resulted in decomposition of the perovskite *B*-site ordered material consistent with the inability to stabilize this structure in air.

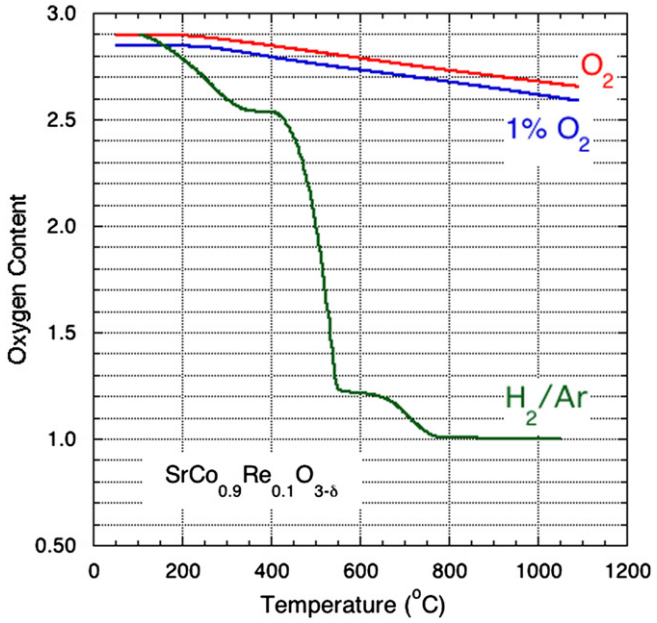

Fig. 2. Thermogravimetric analysis of $SrCo_{0.9}Re_{0.1}O_{3-\delta}$ performed in various atmospheres.

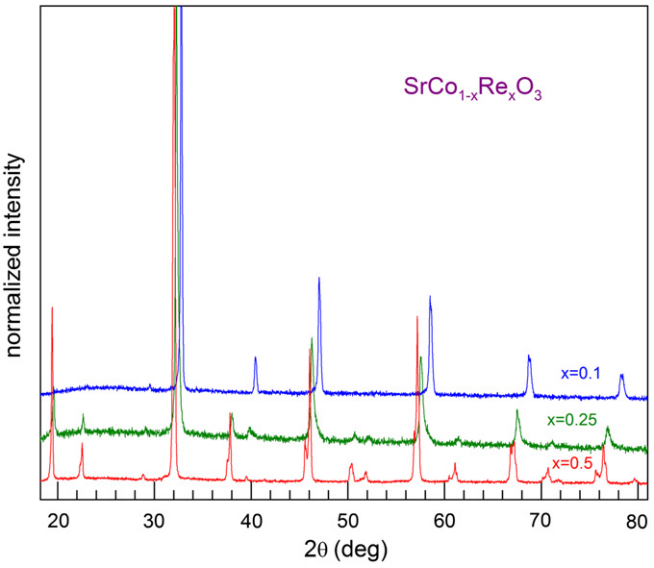

Fig. 3. Room temperature X-ray diffractograms for maximally oxidized $SrCo_{1-x}Re_xO_{3-\delta}$ (x=0.1, 0.25 and 0.5) samples.

Despite being a mixture of two phases, the $x=0.25$ sample was found to be oxygen stoichiometric ($\delta=0.00$) after cooling in oxygen indicating that the disordered phase present in this sample has the Re content x higher than 0.1; thus, allowing its complete oxygenation. Taken together with the previously depicted Re content $x<0.5$ for the *B*-site ordered phase these observations indicate the existence of a miscibility gap and phase separation to compositions $x=xd$ and $x=xo$ with disordered and ordered structures, respectively, with $xd>0.1$ and $xo<0.5$ where both values of xd and xo can be slightly altered by the synthesis procedures.

For a precise crystal structure determination of $SrCo_{1-x}Re_xO_3$ ($x=0.1$, 0.5), time of-flight neutron powder diffraction data were collected at room temperature on the special environment powder diffractometer SEPD [29] at the intense pulsed neutron source of Argonne National Laboratory. High-resolution back-scattering data (detector bank 1, $2\theta=144.85^\circ$) were analyzed using the Rietveld method with the GSAS (EXPGUI) suite [30]. For $SrCo_{0.75}Re_{0.25}O_3$, constant wavelength neutron diffraction data were collected over a wide angular range of $15^\circ<2\theta<159^\circ$ in 0.050° steps using a wavelength of 1.622 Å on the high resolution powder diffractometer Echidna at the OPAL reactor of the Australian Nuclear Science and Technology Organization (ANSTO).

Magnetization measurements were performed in a physical property measurement system (Quantum Design) for $x=0.1$, 0.5 and in a magnetic property measurement system (also Quantum Design) for $x=0.25$. Prior to the measurements, the samples were cooled to 5 K in a zero magnetic field. At 5 K, a magnetic field $H=1$ kOe was established and the "zero-field-cooled" magnetization curves were measured while the temperature was being swept from 5 to 390 K. "Field-cooled" magnetization measurements were performed on cooling in the same magnetic field down to 5 K. Then, the magnetic field was turned off and the thermoremanent magnetization was measured on warming.

Electrical and thermal transport properties were studied in a physical property measurement system equipped with a thermal transport option, in the temperature range 10–390 K.

3. Structural properties

Room temperature X-ray diffractograms for maximally oxidized $SrCo_{1-x}Re_xO_{3-\delta}$ ($x=0.1$, 0.25 and 0.5) samples are shown in Fig. 3. Inspection of the XRD patterns shows that the relative peak positions and intensities strongly change with rhenium doping (x-level). In the following paragraphs, we will start our discussion with the single phase $x=0.1$ and 0.5 compositions before we turn our attention to the biphasic $x=0.25$ sample.

3.1. $SrCo_{0.9}Re_{0.1}O_{3-\delta}$

Thermogravimetric measurements for the sample with the lowest rhenium content ($x=0.1$) have shown that oxygen stoichiometry is controlled by the atmosphere maintained during the final firing. As shown in Fig. 4, single-phase $SrCo_{0.9}Re_{0.1}O_{3-\delta}$ samples were obtained having oxygen deficiencies that vary between 0.06 and 0.48. The absence of any all odd Miller indexed reflections in X-ray diffraction patterns, if a double cubic unit cell is used, suggests that the *B*-site cations are disordered, as expected. All peaks were preliminarily indexed using a typical cubic perovskite unit cell with space group *Pm*-3*m*. The lattice parameter a obtained from Rietveld refinements increases from 3.8583(2) Å for the maximally oxygenated sample ($\delta=0.06$) to 3.9167(3) Å for the sample with $\delta=0.48$ (see inset of Fig. 4) consistent with the decreasing average valence of the cobalt ions from 3.53+ to 2.6+ assuming the Re valence of 7+, commonly found in materials with similar compositions or structures [31].

Possible reduction of the cubic symmetry to tetragonal as a result of the progressive tilting of BO_6 octahedra might induce small shifts of the oxygen atoms, which could be observed by neutron diffraction. Thus to obtain more detailed information about the crystal structure of $SrCo_{0.9}Re_{0.1}O_{2.94}$ ($\delta=0.06$) the time-of-flight neutron powder diffraction were examined. Careful examination of NPD profile did not reveal any superstructure peaks or additional splitting of the main perovskite diffraction line. Refinement of the average crystal structure on the basis of a primitive cubic perovskite (*Pm*-3*m*) gave an overall fit with reasonable agreement factors $R_{wp}=5.5\%$ and $\chi^2=1.79$.

The observed, calculated and difference patterns of $SrCo_{0.9}Re_{0.1}O_{2.94}$ are displayed in Fig. 5. Structural parameters are listed in

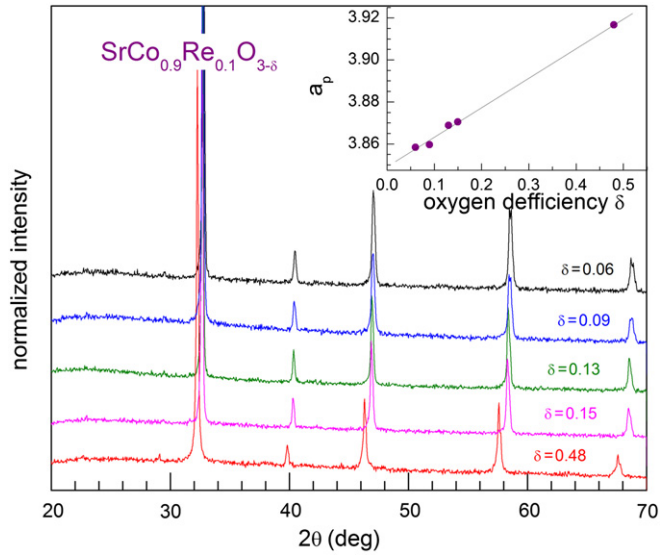

Fig. 4. X-ray diffraction patterns for $SrCo_{0.9}Re_{0.1}O_{3-\delta}$ samples with different oxygen deficiencies. The inset shows cubic lattice parameter a_p obtained from Rietveld refinement as a function of δ.

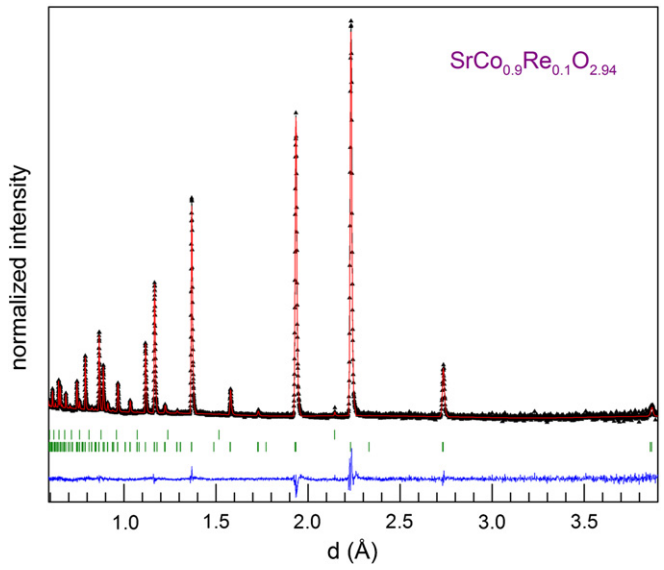

Fig. 5. Neutron diffraction pattern for $SrCo_{0.9}Re_{0.1}O_{2.94}$. Experimental data points are presented as triangles. The continuous lines are the refined patterns and differences between the data and the refined patterns. Intensity peak positions are marked as short vertical lines for the $Pm-3m$ and the vanadium can structure from top to bottom.

Table 1. The refined oxygen occupancies $g_O=0.984(4)$ give a total oxygen stoichiometry of ~2.95 in good agreement with the TGA-determined value.

In the Pm-3m model, the regular $(Co/Re)O_6$ octahedra are composed of six identical (Co/Re)-O bonds of 1.93173(18) Å, in accordance with other compounds containing mixtures of Co(III) and Co(IV), which agrees well with the expected average bond-length calculated as the sum of ionic radii for Re^{7+}–O in octahedral coordination ($\langle {}^{VI}Re^{7+}\text{–}O\rangle = 1.93$ Å), Co^{4+}–O in a high spin (HS) configuration ($\langle {}^{VI}Co^{4+}\text{–}O\rangle = 1.93$ Å) and Co^{3+}–O in a low spin (LS) configuration ($\langle {}^{VI}Co^{3+}\text{–}O\rangle = 1.945$ Å) [32]. The average valence of Co is 3.53+, which gives the Co^{4+}/Co^{3+} ratio close to 1. A typical Sr–O bond length of 2.73187(18) Å is obtained in agreement with twelve coordinated strontium in similar oxides [17,21].

Table 1
Crystallographic parameters, atomic positions, thermal parameters, and reliability factors from the Rietveld refinements for $SrCo_{0.9}Re_{0.1}O_{2.94}$.

Atom	Site	*x*	*y*	*z*	*B*	Oc.
Sr	1*b*	0.5	0.5	0.5	1.202(33)	1
Co/Re	1*a*	0	0	0	0.58(5)	0.901(3) /0.099(3)
O	3*d*	0.5	0	0	1.572(24)	0.984(4)

Space group Pm-3m.
$a=3.8635(4)$ Å.
Reliability factors: $\chi^2=1.79$ $Rw_p=5.5\%$, $R_p=3.93\%$.

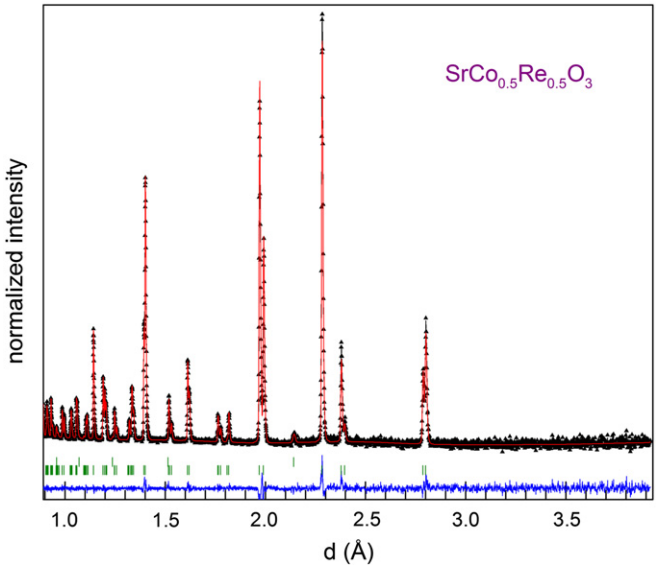

Fig. 6. Neutron diffraction pattern for $SrCo_{0.5}Re_{0.5}O_3$. Experimental data points are presented as triangles. The continuous lines are the refined patterns and differences between the data and the refined patterns. Intensity peak positions are marked as short vertical lines for the vanadium can and the $I4/m$ structure from top to bottom.

3.2. $SrCo_{0.5}Re_{0.5}O_3$

For this sample, several significant superlattice lines were observed and indexed using a doubled cubic unit cell, suggesting the ordering of the CoO_6 and ReO_6 octahedra. A close examination of the main peak splitting showed that the space group $I4/m$ is suitable to fit the data as previously demonstrated by Retuerto et al. [27]. For convenience, the chemical formula for this ordered structure may well be written as Sr_2CoReO_6. The observed, calculated, and difference neutron diffraction patterns are shown in Fig. 6. Crystallographic data and characteristic inter-atomic distances are listed in Tables 2 and 3, respectively. Our results are in a very good agreement with those reported in Ref. [27], where hexavalent Re and divalent Co ions were suggested. The refined oxygen occupancy is close to 3.00 in agreement with the TGA measurements. An average $\langle$Co–O$\rangle$ bond length of 2.0629 Å was obtained consistent with other oxides containing Co^{2+} [27] and in agreement with the Co^{2+}–O bond length calculated using Shannon's tables for the ionic radii [32] for six coordinated LS cobalt ions (2.05 Å). An average Re–O bond length of 1.910 Å was obtained in agreement with 1.920 Å obtained by Kato et al. [26] and Retuerto et al. [27] for Sr_2CoReO_6 and slightly smaller than the expected value for Re^{+6}–O (1.95 Å) calculated using Shannon's tables [32].

Table 2
Crystallographic parameters, atomic positions, thermal parameters, and reliability factors from the Rietveld refinements for $SrCo_{0.5}Re_{0.5}O_3$.

Atom	Site	x	y	z	B	Oc.
Sr	4d	0	0.5	0.25	1.143(28)	1
Co	2b	0	0	0.5	1.66(17)	1
Re	2a	0	0	0	0.03(7)	1
O	4e	0	0	0.2409(3)	B_{11}=1.97(9), B_{22}=1.97(9), B_{33}=0.76(11)	1
O	8h	−0.2706(3)	0.2092(3)	0	B_{11}=0.43(14), B_{22}=1.43(12), B_{33}=2.18(9), B_{12}=0.56(8)	1

Space group *I*4/*m*.
a=5.5715(7) Å, c=7.9594(11) Å.
Reliability factors: χ^2=1.39 Rw_p=5.67%, R_p=3.99%.

Table 3
Selected inter-atomic distances for $SrCo_{0.5}Re_{0.5}O_3$.

Bond	Multiplication	Distance (Å)
Sr–O(1)	(×4)	2.78674(6)
Sr–O(2)	(×4)	2.97661(5)
Sr–O(2)	(×4)	2.63630(4)
⟨Sr–O⟩		2.7999
Re–O(1)	(×2)	1.91818(4)
Re–O(2)	(×4)	1.90596(4)
⟨Re–O⟩		1.9100
Co–O(1)	(×2)	2.06161(5)
Co–O(2)	(×4)	2.06355(4)
⟨Co–O⟩		2.0629

3.3. $SrCo_{0.75}Re_{0.25}O_3$

The XRD pattern of the intermediate composition $SrCo_{0.75}Re_{0.25}O_3$ looks somewhat similar to the one obtained for $SrCo_{0.5}Re_{0.5}O_3$ except for the lower intensities of the superlattice lines together with some peak broadening. Based on basic in-house X-ray measurements, Nag et al. [28] have argued that $SrCo_{0.75}Re_{0.25}O_3$ forms a double perovskite superstructure (*Fm*-3*m*) in response to *B*-site cationic ordering. Our repeated attempts to refine this model using X-ray and neutron data were not satisfactory giving relatively poor agreement factors ($\chi^2 > 2$). The tetragonally distorted *I*4/*m* superstructure was not suitable either albeit with better agreement factors (χ^2=1.76). In both models, many peaks remained poorly fitted.

Questioning the non-suitability of both superstructures and noting the observed peak broadening, we next examined the behavior of the all-even/all-odd Miller indexed reflections for the sample after subjecting it to various post annealings in argon (oxygen deficient) (Fig. 1b) and pure oxygen (fully oxygenated) (Fig. 1a). As shown in Fig. 1, the all-even *hkl* reflections shift to higher 2θ values after oxygenation whereas the *R*-point all-odd *hkl* reflections (along the same all even crystallographic directions) remain clearly unaffected. This observation clearly demonstrates that the $SrCo_{0.75}Re_{0.25}O_3$ sample must be a mixture of two phases. The first phase (disordered perovskite with $x \sim 0.1$) with variable oxygen content is responsible for the fundamental perovskite peak shifts while the second phase (ordered perovskite with $x \sim 0.5$) with fixed oxygen content, irrespective of post-annealing conditions, produces the unchanging *R*-point reflections. Superposition of these diffraction patterns may be easily confused with partial *B*-site ordering of the cobalt and rhenium cations for the oxygen deficient x=0.25 sample. Rietveld refinements show the lattice parameter of the first phase to decrease slightly from 3.9253(4) Å to 3.9207(3) Å with increasing oxygen content. This change is similar to the one observed for the x=0.1 sample; however, the smaller magnitude of the change together with the larger lattice constants point to a Re content (xd) higher than 0.1 of the disordered phase. Our results clearly indicate that $SrCo_{0.75}Re_{0.25}O_{3-\delta}$ compositions form as mixtures of disordered $SrCo_{1-xd}Re_{xd}O_{3-\delta}$ (*Pm*-3*m*, $xd > 0.1$) and ordered $SrCo_{1-xo}Re_{xo}O_3$ (*I*4/*m*, $xo < 0.5$) and suggest the presence of a miscibility gap.

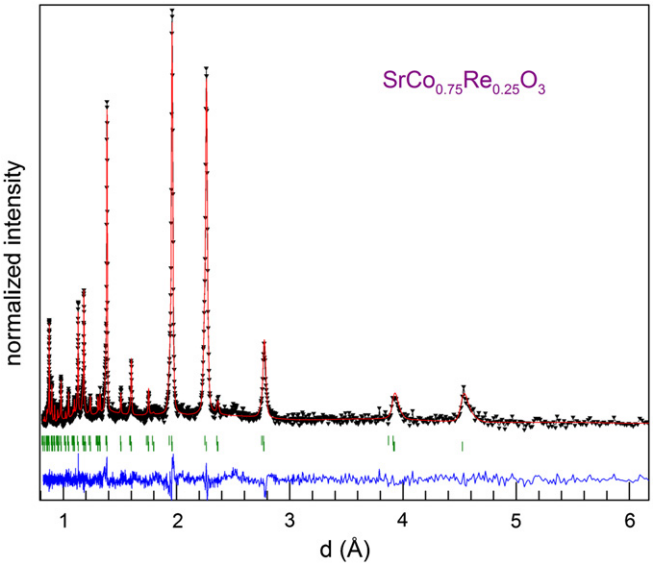

Fig. 7. Neutron diffraction pattern for $SrCo_{0.75}Re_{0.25}O_3$. Experimental data points are presented as triangles. The continuous lines are the refined patterns and differences between the data and the refined patterns. Intensity peak positions are marked as short vertical lines for the *I*4/*m* structure and *Pm*−3*m* structure from top to bottom.

Rietveld refinements using NPD data were carried out for the fully oxygenated $SrCo_{0.75}Re_{0.25}O_3$ sample by taking as the starting model a two-phase mixture (*Pm*-3*m* and *I*4/*m*) proven appropriate for $SrCo_{0.9}Re_{0.1}O_3$ and $SrCo_{0.5}Re_{0.5}O_3$, respectively. The refinement led to a reasonable fit with agreement factors χ^2=1.12 and weight percentages of 65% and 35% for the disordered *Pm*-3*m* and ordered *I*4/*m* phases, respectively. In agreement with XRD, the refined lattice parameters a=3.8910(7) Å for the disordered *Pm*-3*m* phase are larger than those obtained with $SrCo_{0.9}Re_{0.1}O_3$ confirming the preliminary conclusion of a higher rhenium content ($xd > 0.1$) for this phase. Additionally, the lattice parameters a=5.5370(4) Å and c=7.8463(13) Å obtained for the ordered *I*4/*m* phase are smaller than those obtained for the $SrCo_{0.5}Re_{0.5}O_3$ sample again in agreement with a lower rhenium content ($xo < 0.5$). In subsequent refinement cycles (χ^2=1.09) the *B*-site occupation factors were refined giving 69% of the $SrCo_{0.88}Re_{0.12}O_3$ phase (xd=0.12) and 31% of the $SrCo_{0.54}Re_{0.46}O_3$ phase (xo=0.46), which results in an overall composition slightly deviated from the nominal $SrCo_{0.75}Re_{0.25}O_3$. However, considering the strong peak overlap of both phases these values should be considered as rough estimates. Thus, the existence of two-phase

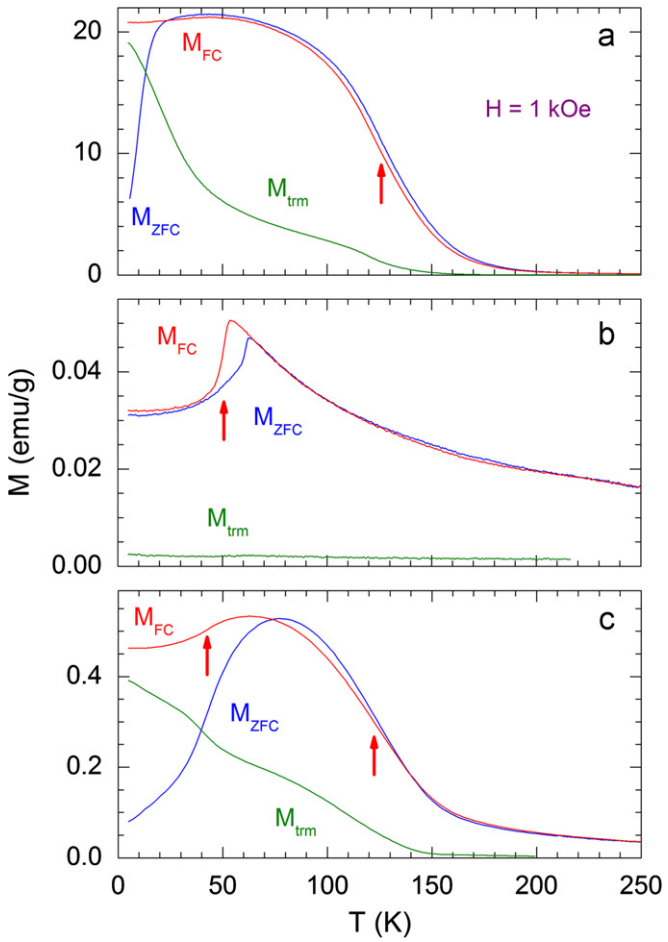

Fig. 8. "Zero-field-cooled" (M_{ZFC}), "field-cooled" (M_{FC}), and thermoremanent (M_{trm}) magnetizations for $SrCo_{1-x}Re_xO_{3-\delta}$ samples: (a) x=0.1, (b) x=0.5, and (c) x=0.25. Arrows denote the magnetic transitions discussed in the text.

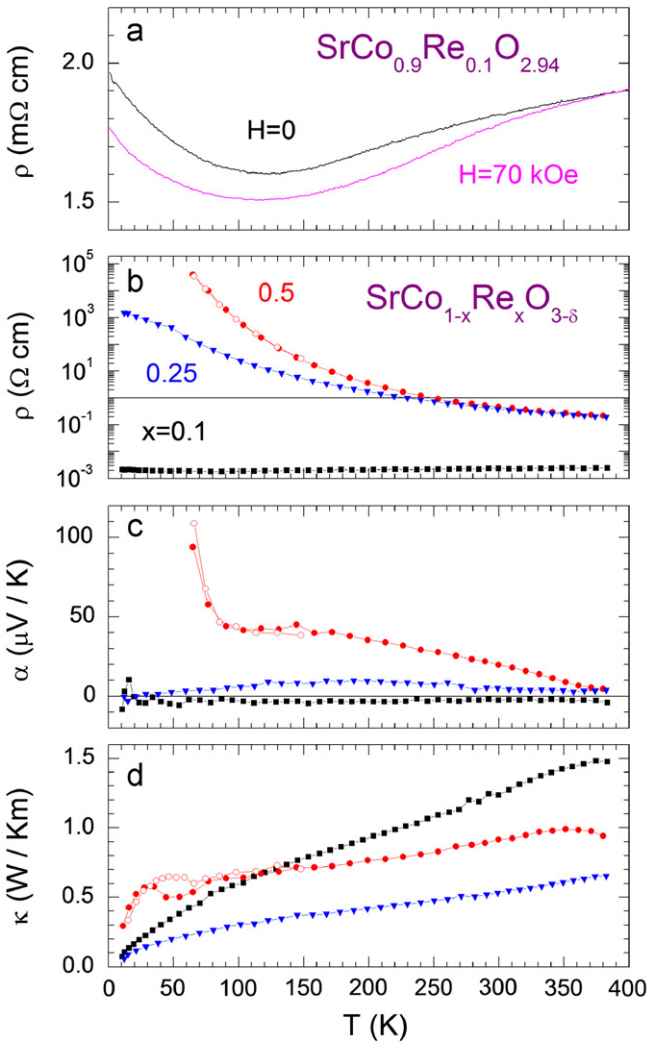

Fig. 9. Electronic and thermal transport properties of $SrCo_{1-x}Re_xO_{3-\delta}$: electrical resistivity (r), the Seebeck coefficient (a), and thermal conductivity (k).

region near $x\sim0.25$ is associated with the segregation to the Pm-3m phase in which the Co and Re ions are randomly distributed on the B site and the Re-rich phase ($I4/m$) where Co and Re are completely ordered with a small amount of antisite Co defects on Re sites. Observed and calculated neutron diffraction intensities together with their difference curve are shown in Fig. 7.

4. Physical properties

4.1. Magnetism

The "zero-field-cooled" (M_{ZFC}), "field-cooled" (M_{FC}) and thermoremanent (M_{trm}) magnetizations are presented in Fig. 8. For $SrCo_{0.9}Re_{0.1}O_{2.94}$, a ferromagnetic behavior can be observed with T_C=125 K determined from the mid-point of the magnetic transition (the point marked with an arrow in Fig. 8(a)). M_{FC} is almost flat at low temperatures, which is expected for a ferromagnetic material. For the x=0.5 sample, both M_{ZFC} and M_{FC} exhibit a sharp step consistent with the antiferromagnetic ordering at a transition temperature T_N, which is different whether the magnetization is measured on warming (61 K) or cooling (51 K). This sharp change of magnetization with a thermal hysteresis is characteristic of a first order transition and is likely coupled with a structural transition, possibly to a monoclinic phase observed for Sr_2CoReO_6 at low temperatures [27]. Further neutron diffraction studies at low temperatures should resolve this issue. M_{trm} is close to zero as expected for the antiferromagnetic order. Practical absence of the thermoremanent magnetization indicates no ferromagnetic contribution (e.g., associated with spin canting) to the antiferromagnetically aligned spins. Magnetic behavior of the x=0.25 sample is more complicated. The ferromagnetic transition at T_C=123 K (almost same as for $SrCo_{0.9}Re_{0.1}O_{2.94}$) is observed, but a significant decrease in M_{FC} can be observed below T_C. The temperature of this drop (42 K) is slightly lower than T_N for the x=0.5 sample observed on cooling. The presence of both ferromagnetic with reduced T_C than observed for the x=0.1 sample and antiferromagnetic transitions with reduced transition temperature than observed for the x=0.5 sample supports our above findings that $SrCo_{0.75}Re_{0.25}O_3$ is a mixture of two structural phases, one similar to $SrCo_{1-xd}Re_{xd}O_3$ and the other to $SrCo_{1-xo}Re_{xo}O_3$ where $xd>0.1$ and $xo<0.5$.

4.2. Electronic and thermal transport

Temperature dependences of the electrical resistivity ρ, the Seebeck coefficient α and thermal conductivity κ are presented in Fig. 9. Electrical resistivity for the x=0.1 sample (Fig. 9(a)) demonstrates metallic-like temperature dependence. A moderate negative magnetoresistance effect can be observed at temperatures

below T_C similar to other metallic oxides like $SrRuO_3$ and ferromagnetic semiconductors like (Ga,Mn)As. The maximum magnetoresistance is close to 10%. Thermal conductivity for the $x=0.1$ sample is roughly linear with temperature and is the highest of all the studied compositions at $T\sim390$ K. The Seebeck coefficient is very small (<5 μV/K), which is characteristic of metallic materials, and negative, suggesting electron doping of this sample. For the $x=0.5$ sample, the Seebeck coefficient is significantly larger and positive. Both α and κ show clear anomalies around the antiferromagnetic transition at temperatures 40–60 K, which is an indication of a coupling between the magnetic, electronic and thermal properties in this material. A possible similar anomaly in the electrical resistivity is hindered by the limitations of our measurement system. The thermal conductivity for the $x=0.25$ sample is visibly lower than that for the other two samples, which indicates more pronounced phonon scattering in this sample. The $x=0.25$ sample shows values of ρ and α in between the values for the $x=0.1$ and 0.5 samples.

5. Summary

In summary, we have studied synthesis conditions and structural, magnetic and transport properties of $SrCo_{1-x}Re_xO_{3-\delta}$ ($x=0.1$, 0.25 and 0.5) samples. We have found that $SrCo_{0.9}Re_{0.1}O_{2.94}$ forms in air as a stable *B*-site disordered cubic *Pm*-3*m* phase, which demonstrates metallic like electrical conductivity and becomes ferromagnetic below 125 K. Fully oxygenated $SrCo_{0.5}Re_{0.5}O_3$ forms under reducing conditions and is a tetragonal *I*4/*m* at room temperature with complete ordering of Co^{2+} and Re^{6+} ions equivalent to a double perovskite Sr_2CoReO_6 with a first order antiferromagnetic transition at low temperatures ($\sim$50–60 K) coupled with changes in electronic and thermal transport. We have demonstrated that $SrCo_{0.75}Re_{0.25}O_3$ is not a partially cation ordered $Sr_4Co_3ReO_{12}$ phase, but a mixture of two structural and magnetic phases with disordered $SrCo_{1-xd}Re_{xd}O_3$ and ordered $SrCo_{1-xo}Re_{xo}O_3$ compositions where $xd\approx0.12$ and $xo\approx0.46$. Our results indicate an existence of the miscibility gap, which does not allow homogenous substitution of Re in $SrCo_{1-x}Re_xO_{3-\delta}$ perovskite above $x>xd$. However, substitution of only 10% Re is sufficient to stabilize perovskite structure against decomposition to hexagonal material and allow significant decrease of oxygen vacancy content. Since this material exhibits metallic conductivity it would be interesting to investigate its (as well as less substituted compositions) mix ionic and electronic properties at elevated temperatures.

Acknowledgments

Work at NIU was supported by the NSF-DMR-0706610. Work at Argonne was supported by the U.S. Department of Energy, Office of Science, Office of Basic Energy Sciences, under contract DE-AC02-06CH11357. Work at Institute of Materials Science and Applied Mechanics was supported by Wroclaw University of Technology (grant No. S10057/I19).

References

[1] V.G. Bhide, D.S. Rajoria, G. Rama Rao, C.N.R. Rao, Phys. Rev. B 6 (1972) 1021–1032.
[2] R.R. Heikes, R.C. Miller, R. Mazelsky, Physica 30 (1964) 1600–1608.
[3] A. Mineshige, M. Inaba, T. Yao, Z. Ogumi, K. Kikuchi, M. Kawase, J. Solid State Chem. 121 (1996) 423–429.
[4] M.A. Senārís-Rodríguez, J.B. Goodenough, J. Solid State Chem. 118 (1995) 323–336.
[5] A.D. Lozano-Gorrın, J.E. Greedan, P. Nunez, C. Gonzalez-Silgo, G.A. Botton, G. Radtke, J. Solid State Chem. 180 (2007) 1209–1217.
[6] T. Nagai, W. Ito, T. Sakon, Solid State Ionics 177 (2007) 3433–3444.
[7] W. Harrison, S.L. Hedwood, A.J. Jacobson, J. Chem. Soc. Chem. Commun. (1995) 1953–1954.
[8] P.D. Battle, T.C. Gibb, A.T. Steel, J. Chem. Soc. Dalton Trans. (1987) 2359–2363.
[9] P.D. Battle, T.C. Gibb, J. Chem. Soc. Dalton Trans. (1987) 667–671.
[10] P.D. Battle, T.C. Gibb, A.T. Steel, J. Chem. Soc. Dalton Trans. (1988) 83–87.
[11] V.V. Vashook, M.V. Zinkevich, Y.G. Zonov, Solid State Ionics 116 (1999) 129–138.
[12] C. de la Calle, A. Aguadero, J.A. Alonso, M.T. Fernández-Díaz, Solid State Sci. 10 (2008) 1924–1935.
[13] X.L. Wang, H. Sakurai, E. Takayama-Muromachi, J. Appl. Phys. 97 (10M519) (2005) 1–3.
[14] Z.Q. Deng, W.S. Yang, W. Liu, C.S. Chen, J. Solid State Chem. 179 (2006) 362–369.
[15] P. Bezdicka, A. Wattiaux, J.C. Grenier, M. Pouchard, P. Hagenmuller, Z. Anorg. Allg. Chem. 619 (1993) 7–12.
[16] V. Primo-Martin, M. Jansen, J. Solid State Chem. 157 (2001) 76–85.
[17] F. Lindberg, S.Ya. Istomin, P. Berastegui, G. Svensson, S.M. Kazakov, E.V. Antipov, J. Solid State Chem. 173 (2003) 395–406.
[18] H. Kruidhof, H.J.M. Bouwmeester, R.H.E. v. Doorn, A.J. Burggraaf, Solid State Ionics 63/65 (1993) 816–822.
[19] K. Yoshii, J. Alloys Compd. 307 (2000) 119–123.
[20] D. Harari, D. Poix, J.D. Bernier, J. Solid State Chem. 11 (1974) 330–339.
[21] A. Aguadero, C. de la Calle, J.A. Alonso, M.J. Escudero, M.T. Fernandez-Diaz, L. Daza, Chem. Mater. 19 (2007) 6437–6444.
[22] Lisheng Chi, A.E.C. Green, R. Hammond, C.R. Wiebe, J.E. Greedan, J. Solid State Chem. 170 (2003) 165–175.
[23] W. Prellier, V. Smolyaninova, A. Biswas, C. Galley, R.L. Greene, K. Ramesha, J. Gopalakrishnan, J. Phys.: Condens. Matter 12 (2000) 965–973.
[24] M. Hanawa, Y. Muraoka, T. Tayama, T. Sakakibara, J. Yamamura, Z. Hiroi, Phys. Rev. Lett. 87 (2001) 187001.
[25] K. Ohgushi, A. Yamamoto, Y. Kiuchi, Ch. Ganguli, K. Matsubayashi, Y. Uwatoko, H. Takagi, Phys. Rev. Lett. 106 (2011) 017001.
[26] H. Kato, T. Okuda, Y. Okimoto, Y. Tomioka, K. Oikawa, T. Kamiyama, Y. Tokura, Phys. Rev. B 69 (2004) 184412.
[27] M. Retuerto, M.J. Martinez-Lope, M. Garcia-Hernandez, M.T. Fernandez-Diaz, J.A. Alonso, Eur. J. Inorg. Chem. 4 (2008) 588–595.
[28] J. Abanti Nag, R.M. Manjanna, Tiwari, J. Gapalakrishnan, Chem. Mater. 20 (13) (2008) 4420–4424.
[29] J.D. Jorgensen, J. Faber Jr., J.M. Carpenter, R.K. Crawford, J.R. Haumann, R.L. Hittermann, R. Kleb, G.E. Ostrowski, F.J. Rotella, T.G. Worlton, J. Appl. Crystallogr. 22 (1989) 321–333.
[30] B.H. Toby, J. Appl. Crystallogr. 34 (2001) 210–213;
A.C. Larson, R.B. von Dreele, General Structure Analysis System, Los Alamos Natl. Lab., LAUR 86-748, 1994;.
[31] S. Kolesnik, B. Dabrowski, J. Mais, M. Majjiga, O. Chmaissem, A. Baszczuk, J.D. Jorgensen, Phys. Rev. B 73 (2006) 214440.
[32] R.D. Shannon, Acta Crystallogr. A 32 (1976) 751–767.